Neuroimage: Reports 2 (2022) 100123

Contents lists available at ScienceDirect

Neuroimage: Reports

journal homepage: www.sciencedirect.com/journal/neuroimage-reports

Brain network for small-scale features in active touch

Saeed Babadi [a], Roger Gassert [b], Vincent Hayward [c], Marco Piccirelli [d], Spyros Kollias [d], Theodore E. Milner [a,*]

[a] Department of Kinesiology and Physical Education, McGill University, Montreal, QC H2W 1S4, Canada
[b] Rehabilitation Engineering Laboratory, D-HEST, ETH Zürich, Zurich, Switzerland
[c] Institut des Systèmes Intelligents et de Robotique, Sorbonne Université, 75005, Paris, France
[d] Clinic of Neuroradiology, University Hospital Zurich, Zurich, Switzerland

ARTICLE INFO

Keywords:
fMRI
Functional connectivity
Perceptual learning
Resting-state network
Somatosensory

ABSTRACT

An important tactile function is the active detection of small-scale features, such as edges or asperities, which depends on fine hand motor control. Using a resting-state fMRI paradigm, we sought to identify the functional connectivity of the brain network engaged in mapping tactile inputs to and from regions engaged in motor preparation and planning during active touch. Human participants actively located small-scale tactile features that were rendered by a computer-controlled tactile display. To induce rapid perceptual learning, the contrast between the target and the surround was reduced whenever a criterion level of success was achieved, thereby raising the task difficulty. Multiple cortical and subcortical neural connections within a parietal-cerebellar-frontal network were identified by correlating behavioral performance with changes in functional connectivity. These cortical areas reflected perceptual, cognitive, and attention-based processes required to detect and use small-scale tactile features for hand dexterity.

1. Introduction

During the dexterous manipulation and exploration of rigid objects, touch can detect many relevant features that are not available to the other senses. Concomitantly, the successful identification of objects by touch relies on the detection of small-scale features that are at the origin of their surface topography and of their structural geometry. In other words, rapid manipulation and object identification fundamentally depend on locating small-scale geometric features such as edges and asperities. In the course of these activities, tactile information guides goal-oriented motor control, while at the same time, specific motor actions enhance accrued tactile information.

Studies which have examined sensorimotor transformations in the coordination of grasping forces (Ehrsson et al., 2003; Schmitz et al., 2005) suggest that updating sensorimotor representations for feedforward control involves a fronto-parietal network, whereas updating for feedback control involves the cerebellum and cingulate cortex. In addition to the primary and secondary somatosensory cortices, areas SI and SII, regions involved in the sensorimotor network include the visual cortex (Ricciardi et al., 2007; Sani et al., 2010), intraparietal sulcus (Bremmer et al., 2001; Wacker et al., 2011), inferior frontal gyrus (Stoesz et al., 2003), prefrontal cortex (Pleger et al., 2006), premotor cortex, supplementary motor area and the cerebellum (Blakemore et al., 1999; Bremmer et al., 2001; van Boven et al., 2005). These regions have been found to show increased activation during the perception of haptic properties.

A recent study on perceptual learning during haptic spatial discrimination suggested that perceptual learning depends on plasticity of perceptual readout by decision processes. Greater activation after training was found in pre-SMA, putamen, cerebellum and thalamic motor nuclei (Sathian et al., 2013). Effective connectivity analysis determined that the majority of paths in which connection weights changed after perceptual learning involved posterior parietal, prefrontal, or subcortical regions implicated in motor and/or decision processes. Therefore, we hypothesized that perceptual learning to actively identify small-scale geometric features in the workspace would require an increase in functional connectivity (FC) between brain areas involved in somatosensory processing and those engaged in motor-related decision processes.

Numerous studies have also shown that brain networks linked to the cerebellum play a major role in the transformation of somatosensory signals into motor commands and in sensorimotor learning (Shadmehr

* Corresponding author.
E-mail address: theodore.milner@mcgill.ca (T.E. Milner).

https://doi.org/10.1016/j.ynirp.2022.100123
Received 22 February 2022; Received in revised form 8 August 2022; Accepted 12 August 2022
Available online 20 August 2022

and Holcomb, 1997; Imamizu et al. 2000, 2003; Nezafat et al., 2001; Ehrsson et al., 2003; Schmitz et al., 2005; Vahdat et al., 2011 Herzfeld et al., 2014; Babadi et al., 2021). Thus, we hypothesized that the functional connectivity (FC) between the cerebellum and regions active during somatosensory processing would increase following tactile perceptual learning.

We analyzed FC in the resting-state network before and after learning to investigate network connections engaged in the transformations from touch to action and action to touch. Our paradigm was based on the well-accepted assumption that, after learning, a remnant connectivity trace remains among the regions of the brain associated with the performance of a sensorimotor task (Albert et al., 2009; Vahdat et al., 2011; van Vugt et al., 2020). To induce rapid tactile perceptual learning, we created a task with a tactile display device that was programmed to render a strip of isolated small-scale tactile features set against a surrounding region populated with similar small scale features. The device could be moved freely for searching. When the scale of the surround features was low compared to the strip, participants could effortlessly locate the strip. However, the search was made increasingly more difficult by increasing the scale of the surround features, hence decreasing contrast. Resting-state fMRI was conducted before and after exploration and learning sessions to identify changes in FC associated with learning. A behavioral performance index quantified the amount of learning and was incorporated into the analysis as a constraint to exclude network connections for which the change in FC was uncorrelated with behavioral performance. This ensured that changes in FC that were unrelated to the perceptual learning task were excluded in the learning network.

2. Materials and methods

2.1. Participants

Sixteen right-hand dominant participants (nine female, seven male, age: 25.2 ± 3.7) with no neurological conditions and no prior experience with the task took part in this study which was approved by the Kantonale Ethikkommission Zürich and conducted in accordance with the Declaration of Helsinki. The study was conducted at the Neuroradiology Clinic of the Universitätspital Zürich. All participants gave written informed consent to the procedures.

2.2. Experimental setup

2.2.1. Apparatus

We employed a high-resolution tactile display that operated on the principle of distributed differential traction on the fingertip skin (Latero, Tactile Labs, Montréal Canada). This device, illustrated in Fig. 1A, delivered fine spatiotemporal tactile stimuli using an 8 × 8 matrix of

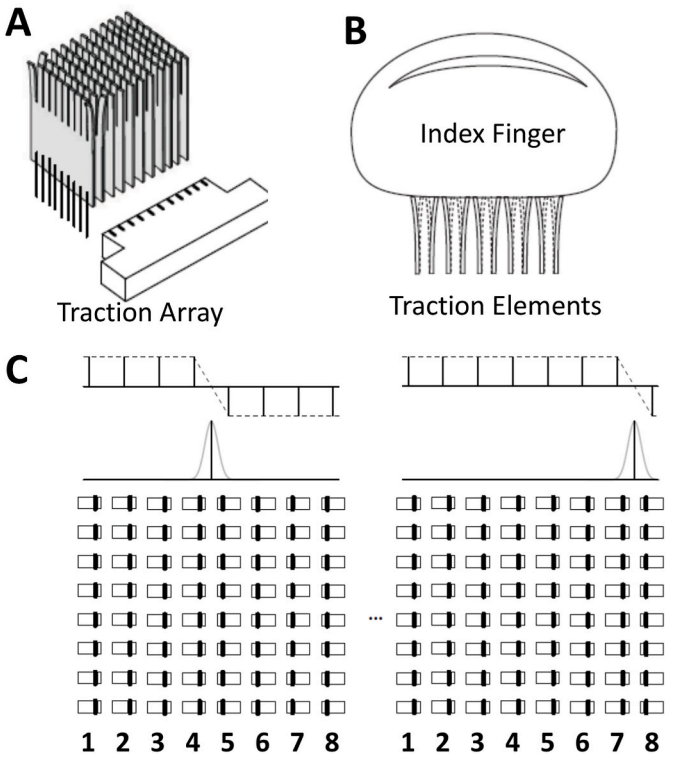

Fig. 2. **A.** Traction array consists of 64 traction elements arranged in an 8 × 8 matrix. **B.** Traction elements can be deflected to the left or right stretching the glabrous skin of the index finger. **C.** Movement of the slider over a distance equal to the spacing of 3 traction columns results in the traction elements of columns 5 to 7 deflecting to the right, creating the illusion of passing over a ridge.

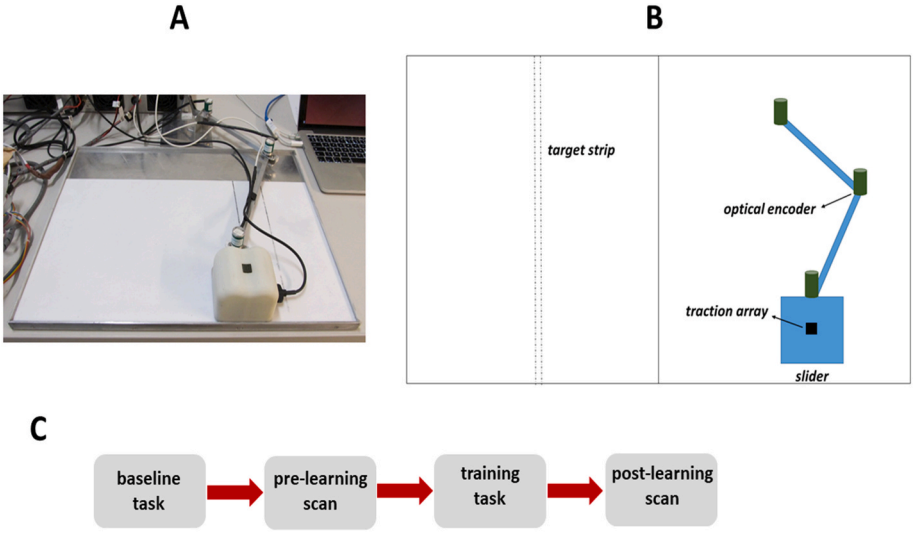

Fig. 1. **A.** Latero (lateral traction array) consists of a mouse-like slider in which traction elements are incorporated and moves over a horizontal surface. **B.** Schematic of the Latero. The black square represents the traction array where the finger is placed. The dashed lines represent a possible location of the target strip. **C.** General experimental protocol and sequence of procedures.

traction elements spaced 1.2 mm apart (Fig. 2A). The display produced subsurface strains in the glabrous skin of the tip of the right index finger (Fig. 2B) by imposing traction gradients at the boundary of the skin within a region of one square centimeter (see Wang and Hayward (2010) for technical details). The Latero display device has been shown to provide vivid and highly repeatable tactile stimuli in a variety of settings (Hayward et al., 2014; Konkle et al., 2009; Petit et al., 2008). The display head, on which the fingertip rested for stimulation, was housed in a contoured slider (8 cm × 6 cm x 10 cm) which glided over a smooth Teflon surface, approximately 30 cm × 20 cm (Fig. 1A). The slider was gripped between the thumb and remaining fingers and moved in a similar fashion to a computer mouse. The position of the display head was measured via a lightweight two-link arm instrumented with high-resolution optical encoders (Fig. 1B). The position data were acquired at 250 Hz.

2.2.2. Stimuli

The activation of the traction elements was controlled in such fashion that the resulting sensation was that of brushing over closely spaced raised features fixed in space not unlike the bristles of a brush. The target stimulus was an 8.4 mm strip oriented along a sagittal axis (Fig. 1B), which was generated by deflecting successive columns of the traction elements as the slider moved over the target strip (Fig. 2C). The amplitude of the commanded deflection of the traction elements was kept constant over the target strip. The amplitude of the deflection outside of the target strip was initially zero but could be increased to create tactile "noise" relative to the tactile "signal" representing the target strip.

2.3. Learning procedure

Each session began with a 5-min baseline task during which participants were instructed to slide the display head back and forth to explore the entire workspace. Vision was occluded by means of opaque ski goggles such that subjects were forced to rely solely on somatosensation to perform all tasks. During an initial baseline exploration task, the features rendered by the traction elements were varied in a random manner as a function of region of the workspace and elapsed time. The objective of the baseline task was to provide the sensation of differences in small-scale tactile features without linking sensation to discrimination or goal-directed movement. Thus, the baseline task provided somatosensory input to the brain without perceptual learning. The baseline task was followed immediately by a pre-learning resting-state fMRI scan which took place in the adjacent MRI suite. The pre-learning scan provided a reference baseline for changes in FC after learning by accounting for the baseline level of functional connectivity related purely to the somatosensory input. The pre-learning scan was followed by a perceptual learning task which was immediately followed by a post-learning resting-state scan aimed to monitor changes in functional connectivity (ΔFC) associated with perceptual learning.

The participants learned to discriminate the strip from the surround by actively searching. A pilot experiment determined that 40% of the maximum deflection was sufficient to unambiguously locate the strip when the deflection in the surround was zero, i.e. when the surround was smooth. This value was kept constant for the target strip throughout training. Participants moved the slider at their preferred speed under the constraint that they locate the target strip within 10 s. They were instructed to stop at the location where they perceived the target strip and if correct, the target strip was randomly moved to a new location 500 ms later. If they did not correctly locate the target strip within 10 s, the trial was designated as unsuccessful and the target strip was immediately moved to a new random location. The new position of the target strip alternated between the left and right half of the workspace. Training was administered in blocks of eight trials. Initially, the traction elements were only deflected over the target strip such that there were no perceived tactile features outside of the target strip. Subsequently, if the participant succeeded in correctly locating the strip for at least five trials within a block, tactile noise was introduced outside the target strip by incrementing the deflection amplitude of the traction elements by 3.125% of their deflection amplitude over the target strip. This reduced the tactile contrast between the target strip and the surround. This allowed for 30 possible tactile noise levels, i.e. ranging from 0 to 90.375% of the deflection amplitude over the target strip (tactile signal). If the participant did not succeed on at least five trials, the tactile noise remained unchanged. The perceptual learning session was divided into two 10-min segments separated by a short break.

2.4. Experimental procedure

Immediately after completing the baseline task, participants underwent a pre-learning fMRI scan in an adjoining MRI suite. This scan reflected the state of the participant's brain, untrained, yet adapted to the stimuli. Upon completion of the pre-learning scan, participants engaged in the perceptual learning task and, thereafter, directly underwent a post-learning fMRI scan. The experimental protocol is summarized in Fig. 1C.

2.5. Behavioral analysis

After having completed N blocks, behavior performance (BP) was quantified by summing the number of successful trials S_i within each block i weighted by a difficulty index D_i, i.e. $\mathrm{BP} = \sum_{1}^{N} S_i D_i$. The difficulty index of a trial was defined as the amplitude of the deflections in the surround relative to that of the target strip. The index was equal to one when the contrast was zero and zero when the contrast was maximum. At regular intervals, the experimenter informed the subject of the performance score to provide motivation. The BP was used in the subsequent FC analyses.

2.6. fMRI protocol

Brain scans were acquired using a 3.0 T S Magnetom Skyra MR scanner at the Neuroradiology Clinic of the Universitätspital Zürich. Participants were in a supine position with their head resting in the head coil in a comfortable position. Foam pads minimized head movements and ear plugs reduced scanner sounds. A simultaneous multi-slice T_2*-weighted EPI sequence (Setsompop et al., 2012; Feinberg and Setsompop, 2013) was used to acquire whole-brain functional data (parallel imaging; 32 head-coil channels; multi-band acceleration factor = 3; spatial resolution 2.75 × 2.75 × 2.75 mm^3, isotropic; slice thickness 2.75 mm, 48 slices; TE = 36.40 ms; TR = 1.10 s). Pre-learning scanning began with a short auto-alignment acquisition, followed by two 8-min resting-state fMRI scans. Participants fixated on a cross displayed inside the scanner and relaxed during resting-state scans. The pre-learning resting-state scans were followed by a 4-min GRE field mapping scan and an 8-min block-design task-based fMRI scan. The purpose of the block-design task was to activate the brain areas involved in haptic identification. Each block consisted of 30 s of the task and 30 s of rest. During the 30 s of the task, a randomly selected object was placed in the palm of the participant's right hand for 6 s and then replaced by another randomly selected object every 6 s. Participants had no prior knowledge of the objects and could not see them. They silently attempted to identify the objects from their shapes and texture. This task alternated with 30 s of rest. The results of the task-based scan were used to determine ROI coordinates of brain regions for functional connectivity analysis. Post-learning scanning was identical to the pre-learning scanning, except that the task-based scan was replaced by a T_1-weighted anatomical scan (spatial resolution 0.94 × 0.94 × 0.94 mm^3, isotropic; slice thickness 0.94 mm; TE = 2.46 ms; TR = 1900 ms).

2.7. fMRI analysis

FSL software packages (FMRIB Software Library v6.0), Oxford, UK (Smith et al., 2004; Jenkinson et al., 2012) were used to process the images. We adapted a method described by Vahdat et al. (2011) to pre-process the resting-state fMRI data using the first-level FEAT toolbox (Woolrich et al., 2001).

The pre-processing pipeline was performed in the following order: five volumes in each scan were removed (to ensure equilibrium magnetization had been reached); non-brain removal using BET (Brain Extraction Tool); motion correction using the 6 DOF rigid body transformation implemented in FLIRT (FMRIB Linear Image Registration Tool); spatial smoothing (Gaussian kernel of FWHM, 5.5 mm); temporal high-pass filtering (Gaussian-weighted least-squares straight-line fitting with $\sigma = 100$ s, equivalent to a cut-off frequency of 0.01 Hz); global intensity normalization.

After the preliminary processing, a regression-based approach was used to model and remove additional artifacts. In addition to the linear motion parameters (three for translations, three for rotations), further motion outliers due to more complex artifacts such as slice by slice changes in motion were detected in the resting-state time series. We used Boundary-Based Registration (BBR) (Greve and Fischl, 2009) and nonlinear registration to obtain spatial transformations between functional and MNI standard space (MNI 152 2 mm brain). The optiBET algorithm (Lutkenhoff et al., 2014) was applied to the T_1-weighted anatomical images to improve brain extraction. Then the extracted T_1-weighted image of the brain of each participant was segmented by FAST (FMRIB's Automated Segmentation Tool), resulting white matter and CSF masks (Fig. S1) were thresholded to ensure 90% tissue type probability and the image was transferred to functional space (Zhang et al., 2001). The average BOLD signals within white matter and CSF masks were calculated and used as confound regressors to remove physiological (cardiac and respiration) noise (Shehzad et al., 2009). Once the regressor confounds, consisting of motion parameters, white matter and CSF, were modeled in a General Linear Model (GLM) on a per participant basis, the residual signal was band-pass filtered (0.01–0.10 Hz) using a 5th-order Butterworth filter with zero-phase lag. The neural activity-related signal in resting-state fMRI was expected to lie within this frequency range (Fox and Raichle, 2007).

2.8. ROI identification

To determine the coordinates of ROIs for later seed-based analysis, we analyzed the task-based fMRI scans. The task-based data were pre-processed as follows: non-brain removal using BET (Brain Extraction Tool); motion correction using the 6 DOF rigid body transformation implemented in FLIRT (FMRIB Linear Image Registration Tool); motion outliers detection; spatial smoothing (Gaussian kernel of FWHM, 5 mm); temporal high-pass filtering (Gaussian-weighted least-squares straight-line fitting with $\sigma = 85$ s); global intensity normalization. A regressor for activity versus the rest condition was modeled with a boxcar function as well as a regressor for the temporal derivative of the task timing, then the two regressors were convolved with a gamma hemodynamic response function. *Z*-score images were obtained from participant-level GLM analysis in FEAT and were then input to the higher-level FEAT for group-level analysis (Woolrich et al., 2004). For the group-level analysis, a mixed-effects model in FEAT with stringent cluster thresholding ($Z > 3.5$, cluster significance threshold of $p = 0.01$, corrected for comparisons using Gaussian random field theory) was used.

We identified and selected ROIs based on the resulting activation maps in the MNI standard space and prior knowledge about sensorimotor learning and processing of somatosensory information. These areas included ipsilateral cerebellum (CB), superior frontal gyrus (SFG), contralateral primary motor cortex (M1), dorsal premotor cortex (PMd), supplementary motor area (SMA), primary somatosensory cortex (SI), secondary somatosensory cortex (SII), posterior parietal cortex (PPC), basal ganglia (BG), visual cortex (VC) and thalamus (TL). Since we observed strong activations in some ipsilateral areas, we added ROIs in ipsilateral PMd, SI, SII and BG. Each ROI was defined as a 5.5 mm-radius sphere with the center located on the peak activity from the group *Z*-score activation maps. We used Harvard-Oxford cortical and subcortical (Desikan et al., 2006), Juelich histological (Eickhoff et al., 2007), probabilistic cerebellar (Diedrichsen et al., 2009) and Oxford-Imanova structural striatal atlases (Tziortzi et al., 2011) to identify anatomical labels of selected seed ROIs. Spatial coordinates of the center of each ROI in MNI standard space, *Z*-value of the peak activity and corresponding anatomical labels are listed in Table 1 and the whole brain activation maps are shown in Fig. 3.

2.9. Functional connectivity analysis associated with behavioral performance

The objective of the functional connectivity (FC) analysis was to investigate the brain networks that were modulated by perceptual learning during a haptic task. We sought to identify the connections between brain areas for which the change in the strength of FC from the pre-to post-training scans, ΔFC, was correlated with BP. The average time series of all voxels in each of the seed ROIs from the pre-processed resting-state data were calculated on a per-participant basis and the correlation between this regressor and any other voxels in the brain was assessed in a participant-level GLM. Since the hemodynamic response function may vary among different subjects, sessions and regions of the brain, the temporal derivative of each seed ROI's regressor was also included in the GLM to take into account possible variations in the hemodynamic delay. After FC analysis at the participant level, a GLM analysis consisting of a mean regressor and a regressor to model the contrast between the pre-learning and post-learning sessions (−1 and 1) was conducted. Finally, group-level analysis was performed across participants using a mixed-effects model ($Z > 2.5$, cluster significance threshold $p = 0.05$, corrected for comparisons using Gaussian random field theory) to generate thresholded *Z*-score FC maps and clusters corresponding to each seed ROI (Woolrich et al., 2004). The lower *Z* threshold of 2.5 for resting-state compared to 3.5 for task-based analysis was required since activity levels in the resting state are much lower than during active performance of a task (Babadi et al., 2021; Vahdat et al., 2011, 2014). In order to identify networks whose FC was modulated by improvement in the task performance, BP was included as an

Table 1
Selected ROIs from a task-based fMRI scan during touching different objects. Each ROI is a sphere with the radius of 5.5 mm whose center is located at the activation peak. The table gives MNI coordinates and *Z* value of center of ROIs as well as anatomical labels. R, right hemisphere; L, left hemisphere.

ROI	Anatomical label	*x*	*y*	*z*	*Z* value
SI	primary somatosensory cortex BA1, L	−44	−28	56	7.53
SI	primary somatosensory cortex BA3b, L	−40	−32	58	6.60
SI	primary somatosensory cortex BA2, R	48	−28	48	6.46
SII	secondary somatosensory cortex OP1, L	−48	−22	18	7.40
SII	secondary somatosensory cortex OP3, L	−38	−6	12	6.51
SII	secondary somatosensory cortex OP1, R	54	−20	16	5.65
CB	cerebellum V, R	4	−62	−16	7.39
CB	cerebellum VI, R	24	−64	−24	6.55
CB	cerebellum VII, R	16	−70	−48	6.52
M1	primary motor cortex BA4, L	−32	−18	66	6.61
PMd	dorsal premotor cortex BA6, L	−34	−14	64	6.61
PMd	dorsal premotor cortex BA6, R	32	−12	62	6.57
SMA	supplementary motor area	−2	−2	58	5.60
PPC	posterior parietal cortex SPL, L	−38	−40	52	5.59
PPC	posterior parietal cortex IPL, L	−56	−22	26	5.64
SFG	superior frontal gyrus, R	18	0	64	5.69
BG	basal ganglia putamen, L	−22	−2	6	7.46
BG	basal ganglia caudate, R	16	18	6	5.65
VC	visual cortex, L	−48	−64	−6	6.53
TL	thalamus, L	−12	−20	4	7.46

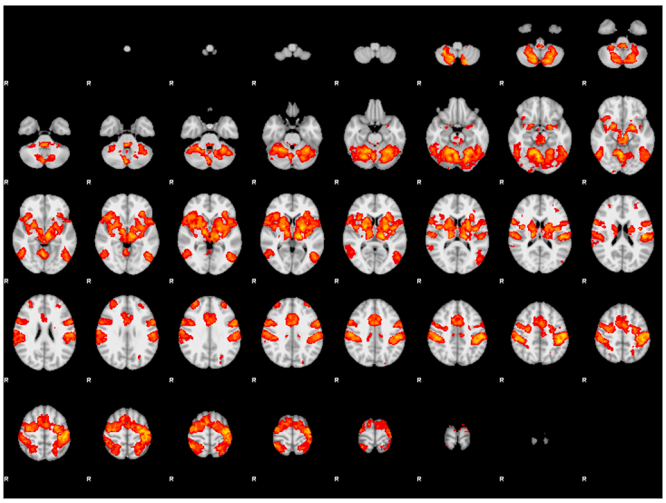

Fig. 3. Whole brain activation maps for the object identification task.

additional regressor in the group-level GLM, as previously described (Vahdat et al., 2011, 2014; Babadi et al., 2021). Correction for multiple comparisons (multiple ROIs) was performed by considering only clusters with p values less than $0.05/20 = 0.0025$ (20 is the number of ROIs) as statistically significant. In addition, we calculated mean absolute values of FC in pre-learning and post-learning sessions and performed linear regression between ΔFC and BP. Only those connections for which there was a statistically significant correlation between BP and ΔFC for individual subjects were retained. Thus, there were two controls for non-specific changes in FC incorporated into the analysis. The first was in the GLM used to find significant changes in FC since BP was incorporated into the GLM and the second was the linear regression. In a previous study (Vahdat et al., 2011) with 13 participants, a difference of at least 90% of baseline FC was found by the effect of motor learning with the standard deviation of 60%. Hence, fourteen participants would provide 90% power at a significance level of 99% ($\alpha = 0.01$) to detect a change in connectivity from pre-to post-learning. To ensure that we had sufficient statistical power in our study, we increased our sample size to 16 participants. Furthermore, in a pilot perceptual learning experiment, involving 10 participants performing similar tactile discrimination, we found a large range in behavioral performance. This ensured that a sample size of 16 participants would also be sufficient to detect statistically significant correlations between FC and BP.

3. Results

Fig. 4 shows the searching movements of one participant in typical trials. The search could begin in either direction, often initially moving away from the target strip. Participants typically searched back and forth with movements of increasing amplitude when they failed to locate the target strip during their initial movement. Occasionally, they were able to stop on the target strip without first completely crossing it, e.g. Fig. 4A. However, for about 90% of the successful trials (984/1085), the target strip was completely crossed at least once, requiring one or more movement reversals before terminating the movement at the correct location. Fig. 5 shows the distribution of number of target strip crossings

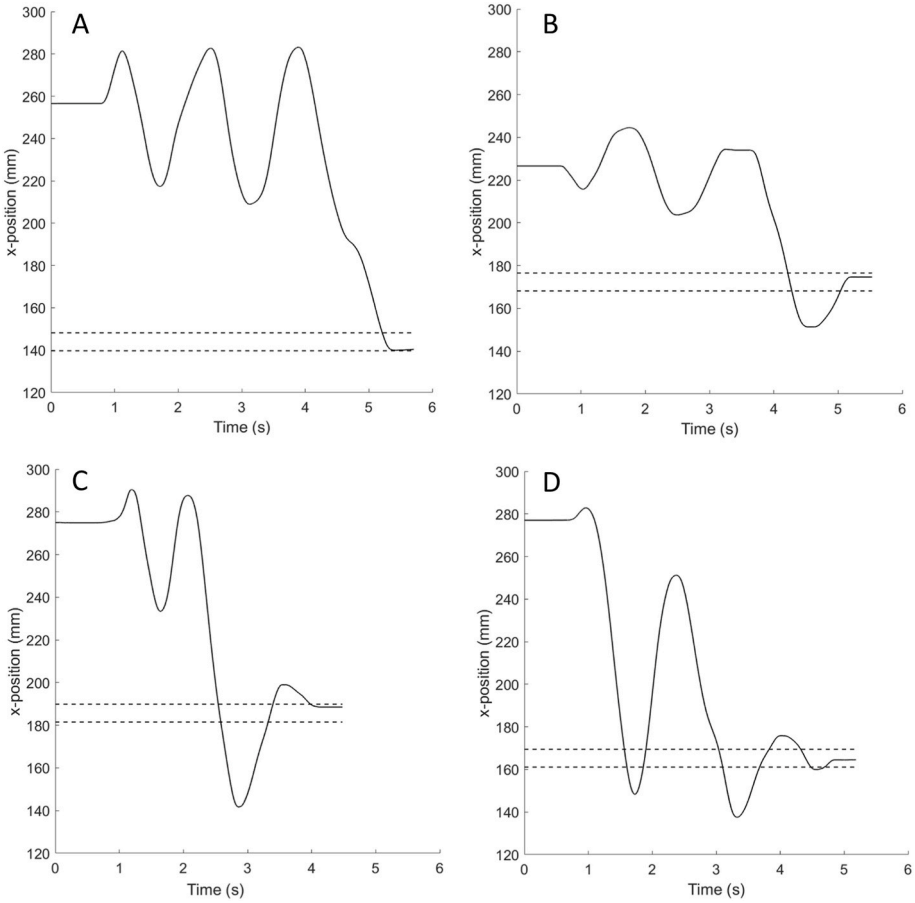

Fig. 4. Representative trials in which the target strip is successfully located. The location of the target strip is displayed by the dashed lines. The x-trajectory of the slider is plotted against time. **A.** Movement stops on the first encounter of the target strip. **B.** Movement stops on the target strip after crossing it and returning. **C.** Movement stops on the target strip after crossing it twice. **D.** Movement stops on target strip after passing over it five times.

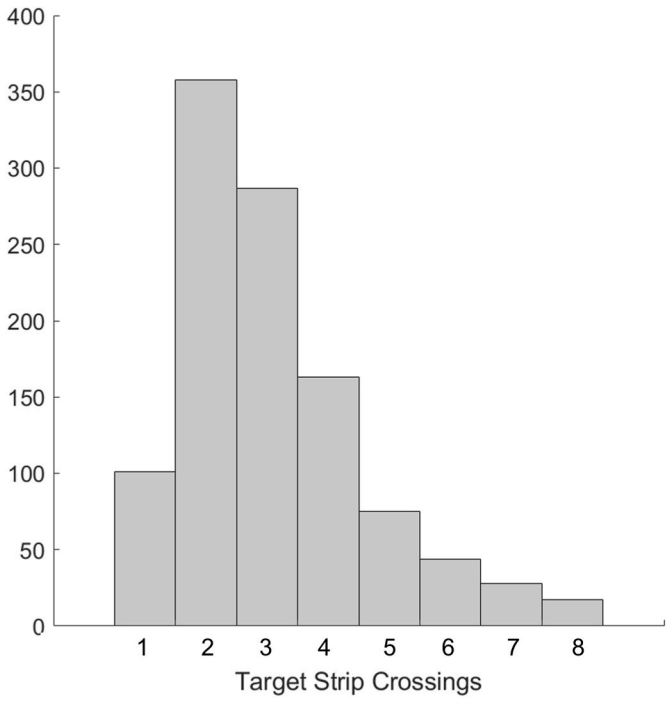

Fig. 5. Histogram of the number of times the target strip was crossed on trials in which the target strip was successfully located within 10 s. A crossing was counted each time the slider entered the target strip. Thus, a value of one represents stopping on the target strip without completely crossing it.

on successful trials. Fig. 6 provides an overview of the relative performance across the group of participants. Almost all participants (14/16) were able to progress beyond the lowest D_i and almost half (7/16) were able to progress to a D_i of 0.375. All participants required more than one trial block, for at least one D_i, to progress to the next D_i. This indicates that learning was required to progress, i.e. no participant reached their final D_i without failures in more than one preceding trial block. The D_i achieved by individual participants ranged from 0 to 0.5625 (mean = 0.348, standard deviation = 0.203), which was significantly greater than zero ($p < 0.00001$). The BP for individual participants ranged from 0 to 1182 (mean = 573, standard deviation = 392), which was also significantly greater than zero ($p = 0.000012$).

The results of the FC analysis are summarized in Table 2 which indicates the clusters corresponding to each ROI, consisting of MNI coordinates and Z value of the peak activity along with significance level

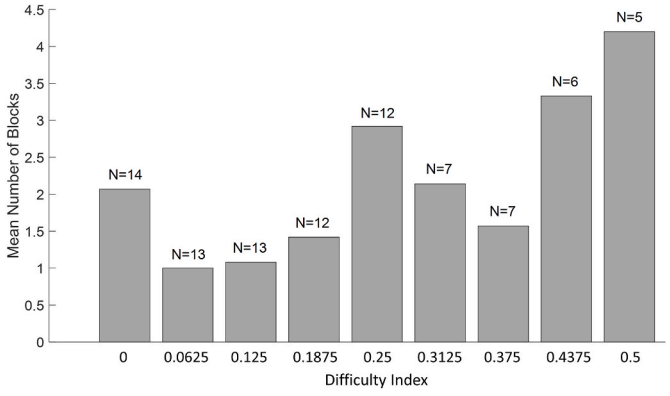

Fig. 6. Histogram of the mean number of blocks completed by each participant for each difficulty index. Blocks were counted only if the participant was able to successfully complete a difficulty index. Numbers at the top of each histogram bar indicate the number of participants who completed each difficulty index.

within each cluster. The top panel in Fig. 7 shows that there was a significant correlation between ΔFC and BP for a neural connection between right PMd and right SI, including regions in both BA1 and BA3b. The FC bar plot shows an increase in the magnitude of connectivity in conjunction with learning. Participants with high BP showed greater ΔFC for this link (regression plot, right panel). Likewise, the middle panel in Fig. 7 shows that ΔFC between SII and bilateral clusters in SI (BA1) increased significantly in relation to BP after training. For these two neural pathways, FC was positive in the pre-learning session and its magnitude increased after training. The bottom panel shows the only negative FC map. It represented a negative correlation between BP and the link between the right SFG and clusters in inferior parietal lobule (IPL) and intraparietal sulcus (IPS). The mean FC decreased from a positive to a less positive value such that subjects with higher BP had greater reduction in FC after training. The upper panel in Fig. 8 shows an increase in FC between cerebellum (lobule VII) and superior parietal lobule (SPL) which was again positively correlated with BP. For this neural pathway, FC was positive in the pre-learning session and its magnitude increased after training. The lower panel in Fig. 8 shows a neural connection between cerebellum (lobule V) and clusters mainly in right amygdala whose ΔFC was also positively correlated with BP. Although the mean FC for this link was initially close to zero, it increased to a significant positive value in the post-learning scan. Fig. 9 depicts the connectivity between brain regions whose functional connectivity was significantly modified by our tactile perceptual learning task.

4. Discussion

Using resting-state analysis, we identified neural substrates of perceptual learning of sensorimotor transformations during active touch. We developed an approach which identified learning-related changes in functional connectivity between brain regions engaged in the transformations between somatosensory inputs and motor commands. Our approach was based on excluding changes in functional connectivity that were uncorrelated with perceptual learning. A baseline exploration task was employed to activate the brain regions engaged by active touch in the absence of learning, which provided baseline functional connectivity in the sensorimotor network. Functional connectivity in the sensorimotor network was again determined after learning to locate a tactile target by active touch as tactile contrast was progressively reduced. By incorporating a behavioral performance (BP) measure to constrain the functional connectivity analysis, we excluded connections to the sensorimotor network for which the change in FC (ΔFC) was uncorrelated with the perceptual learning. This approach enabled us to exclude non-specific changes in functional connectivity and to identify network connections whose ΔFC was highly correlated with perceptual learning.

We found that ΔFC between right (ipsilateral) PMd and SI was positively correlated with BP. The fact that significant correlation was found in the ipsilateral hemisphere merits discussion. There is evidence that neural activation in PMd is generally less lateralized and more effector-independent than in M1 (Cisek et al., 2003). Christensen et al. (2007) found activation in multiple ipsilateral areas during task-based fMRI while interacting with different objects. They proposed that the premotor cortex participated in proprioception by predicting the somatosensory consequences of voluntary movements. It has also been shown that unilateral somatosensory inputs can be processed and represented bilaterally in the left and right SI (Sutherland and Tang, 2006). As task difficulty increased, perceptual training under increasing task difficulty may have necessitated the recruitment of ipsilateral sensorimotor regions in addition to the usual contralateral regions. It was found, for example, that activity in the ipsilateral premotor cortex increases when finger movements become more complex (Rao et al., 1993). If we lower our threshold for statistical significance from Z = 2.5 to Z = 2.3, we do see a change in FC between ipsilateral PMd and both ipsilateral and contralateral SI, although the cluster size in the

Table 2
Summary of the results for the functional connectivity analysis in relation to the performance score. The table gives details of clusters whose functional connectivity significantly changed in conjunction with the behavioral performance (BP) corresponding to each ROI after the training task. Peak *Z* value and MNI coordinates are related to the peak activity of the cluster and *p* cluster is associated with the significance level. Mean FC values across all participants before and after training are also represented. Anatomical labels for ROI and corresponding clusters are given in the first and second columns. PMd, dorsal premotor cortex; SII, secondary somatosensory cortex; CB, cerebellum; SFG, superior frontal gyrus; R, right hemisphere; L, left hemisphere.

ROI	Cluster label	*p* cluster	Peak *Z* value	*x*	*y*	*z*	FC (Pre)	FC (Post)
PMd, R	primary somatosensory cortex BA1 & BA3b; R	1.88×10^{-5}	4.32	40	−18	44	8.64	11.25
SII OP1, L	primary somatosensory cortex BA1; L & R	0.0001	4.38	−46	−24	60	5.09	6.83
CB VII, R	posterior parietal cortex SPL; L	0.0002	5.34	−30	−58	52	3.13	4.99
CB V, R	amygdala; R	7.7×10^{-5}	4.56	14	0	−16	0.22	2.73
SFG, R	inferior parietal lobule PF, anterior intraparietal sulcus; L	0.0001	3.64	−50	−40	38	6.52	3.76

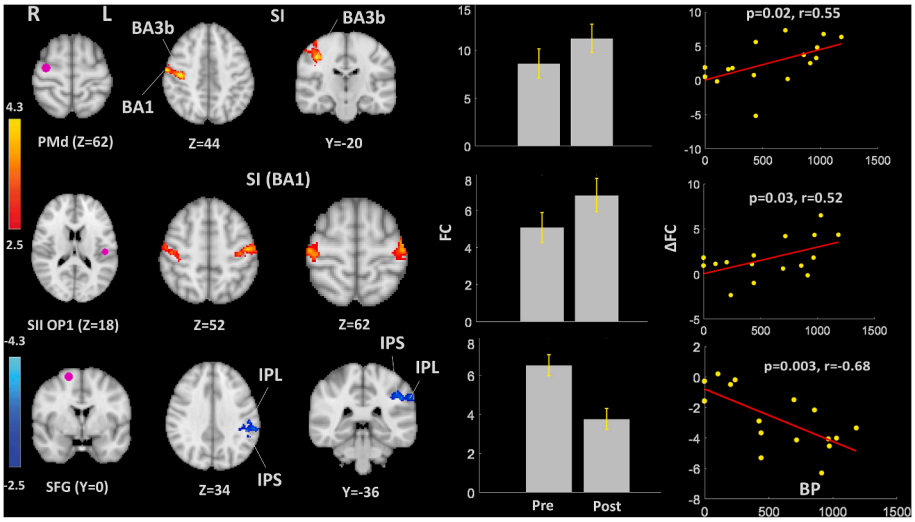

Fig. 7. Functional connectivity (FC) maps in conjunction with the behavioral performance (BP). Each row represents an ROI whose change in FC with other brain areas, from the pre-to the post-training scan, was significantly correlated with the BP. Positive maps are depicted as red to yellow and negative maps are depicted as dark to light blue. Left column shows the location of the ROI displayed as a magenta dot. The second and third columns show the cluster locations of the functionally connected regions. The fourth column shows the mean and standard error of FC values averaged across all subjects. The last column shows the linear regression between change in the FC (ΔFC) and BP on a per-subject basis with the significance level *p* and the Pearson correlation coefficient *r*. PMd, dorsal premotor cortex; SFG, superior frontal gyrus; IPL, inferior parietal lobule; IPS, intraparietal sulcus; R, right hemisphere; L, left hemisphere. (For interpretation of the references to colour in this figure legend, the reader is referred to the Web version of this article.)

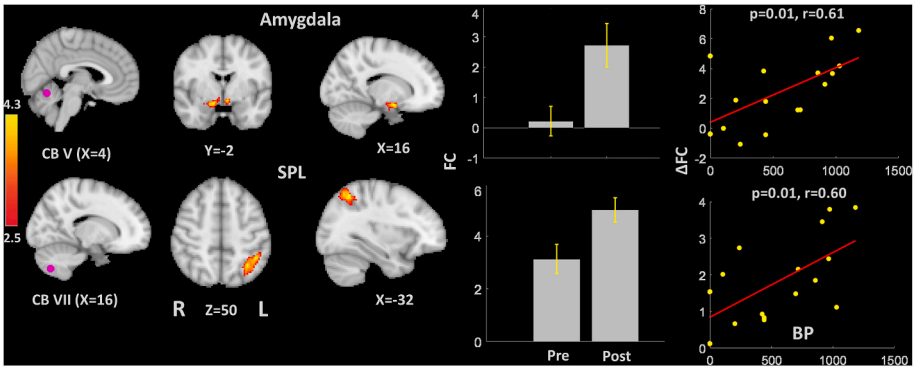

Fig. 8. Functional connectivity maps for ROIs in the right cerebellum (CB). SPL, superior parietal lobule.

contralateral hemisphere is approximately 30% of the cluster size in the ipsilateral hemisphere. This suggests that ΔFC between premotor and primary sensory areas in the ipsilateral hemisphere are vital for discrimination of increasingly small differences in tactile features.

Changes in neural activity in PMd have been implicated in decision making during movement planning for action selection, both in visual (Thura and Cisek, 2014) and somatosensory discrimination tasks (Rossi-Pool et al., 2017). Thus, the identification of a link between SI and PMd was consistent with our second hypothesis, namely that functional connectivity would increase between brain areas involved in somatosensory processing and areas engaged in motor decision processes. Areas BA1 and BA3b of SI are key for first-level processing of tactile information. Increased functional connectivity between ipsilateral SI and PMd was likely related to perception of the target strip since subjects who could perceive smaller differences in tactile features between the target and background (higher BP scores) showed greater changes in functional connectivity. It is likely that the change in functional connectivity was related to adjustments in perceptual sensitivity such that higher performing subjects were able to amplify somatosensory inputs to PMd by increasing functional connectivity. In this way, the perceptual readout by motor decision processes would have been reweighted, as suggested by Sathian et al. (2013), allowing subjects to decide when a difference in tactile features was encountered. Those subjects who were able to detect smaller differences in tactile features demonstrated the greatest reweighting, i.e. the largest change in functional connectivity.

Functional connectivity between SI (area BA1) and SII (area OP1) increased after training. The participants who performed the task successfully for the smallest contrast also had the greatest ΔFC. We did not

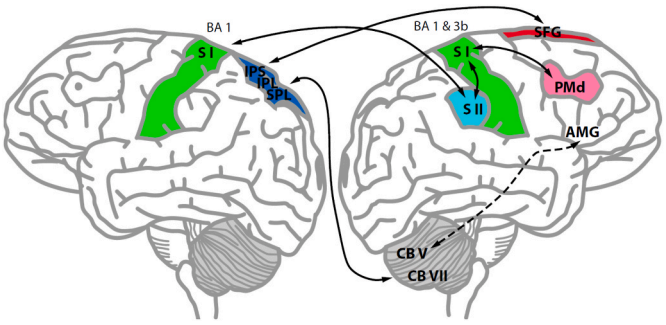

Fig. 9. Connectivity between seed ROIs and brain regions for which changes in functional connectivity were correlated with behavioral performance, comprising a network for detecting small-scale tactile features in active touch.

anticipate, however, that functional connectivity between SII and SI would increase bilaterally. The analysis could not distinguish whether projections from SI to SII or from SII to SI were responsible for ΔFC. The right SI would have received minimal sensory input since the task was performed with the right hand. Therefore, ΔFC between the left SII and right SI must have been due to callosal projections (Manzoni et al., 1986). On the other hand, ΔFC between the left SII and the left SI may have involved ipsilateral and contralateral pathways. It is likely that functional connectivity from SI to SII increased as the task became more difficult since SII was expected to participate in tactile discrimination (Jiang et al., 1997; Pleger et al., 2003), along with attentional modulation (Hsiao et al., 1993), and past sensory history (Romo et al., 2002). It is also possible that functional connectivity from SII to SI might have increased to enhance the information being supplied by SI back to SII.

Consistent with the anatomically documented connection between cerebellum and PPC (Strick et al., 2009) and its potential role in perceptual processing, we found a positive ΔFC between the right cerebellum (lobule VII) and the left SPL. Vahdat et al. (2011) found an increase in functional connectivity between cerebellum and SPL that was dependent on both motor learning and perceptual learning. The prominent dependence of the cerebellum on sensory feedback for error correction (Imamizu et al., 2000) and the significantly greater role of left (contralateral) SPL in tactile localization than recognition (Reed et al., 2005) suggest that functional connectivity between these areas is required for fine sensorimotor control.

In contrast with the above findings, the functional connectivity between the cerebellum (lobule V) and the amygdala was not initially significantly different from zero. An increase in functional connectivity and a strong correlation between ΔFC and BP suggests that the amygdala was progressively recruited during attentional engagement as the search task became more difficult. The amygdala was previously shown to modulate cerebellar learning via somatosensory inputs in rodents (Farley et al., 2016), suggesting a role which involved an attention-based mechanism (Gallagher and Holland, 1994).

The negative correlation between ΔFC and BP for functional connectivity between right SFG and left IPL/anterior IPS indicates that the better participants performed, the more they reduced the strength of this connection. The ROI was centered in the posterior part of SFG (Table 1), which has been identified as belonging to the SMA (Li et al., 2013). Area IPL is thought to be involved in multisensory integration (Binkofski et al., 2016) and visuomotor transformations (Fogassi and Luppino, 2005), particularly in the context of tactile object recognition (Jäncke et al., 2001; Reed et al., 2005). Neurons in the anterior IPS in monkey (Sakata et al., 1995) and human (Frey et al., 2005; Tunik et al., 2005) have been shown to have visual and motor properties suggesting roles related to visuomotor transformations and visual control of dexterous finger movements (Fogassi and Luppino, 2005). It has been shown, through effective connectivity analysis, that connectivity between IPS and SMA is reduced as working memory or cognitive demands increase (Harding et al., 2015). The reduction in functional connectivity between SFG and areas IPL and IPS of the parietal cortex is, therefore, likely due to the cognitive demands required to detect the target strip. Furthermore, higher cognitive demands would be required as the tactile noise in the surround increased relative to the tactile signal representing the target strip, such that participants who achieved higher BP scores would have experienced higher cognitive demands than those who performed less well, explaining the negative correlation (greater reduction in functional connectivity) between ΔFC and BP.

There have been numerous studies of brain areas involved in processing of somatosensory information emanating from the hand, including tactile discrimination. However, these studies do not combine the two defining elements of our study, namely improved tactile discrimination (perceptual learning) with transformation of sensory input to motor output (goal-directed movement). Furthermore, our study differs from studies of motor adaptation, which generally involve a perturbation which alters the sensory signal and requires remapping between sensory input and motor output. In our study, the salient sensory signal (target strip) did not change. Our study design focused on changes in functional connectivity in the resting state that were correlated with perceptual learning. Therefore, it provides an understanding, not only of where sensorimotor transformation takes place, but of how it takes place, i.e. by strengthening functional connections between specific regions of the brain. In particular, we suggest that functional connections between region OP1 of contralateral SII and bilateral SI are strengthened to amplify signals used in high level processing of tactile information. Similarly, we suggest that strengthening of functional connections between ipsilateral PMd and SI represents reweighting of decision processes based on changing somatosensory signals. Strengthening of functional connections between the cerebellum and amygdala likely represents increased attention to small differences in somatosensory signals, necessary as the tactile signal to noise ratio decreases. We suggest that the observed reduction in functional connectivity between the superior frontal gyrus (identified as part of the SMA) and inferior parietal cortex is related to the nature of the task, in which cognitive demands increased as the tactile signal to noise ratio decreased. The magnitude of changes in functional connectivity between nodes in this network (Fig. 9) appears to be directly related to the ability to detect and utilize small-scale tactile features to guide dexterous manipulation.

Data and code availability statement

MRI data are not available because of ethical considerations. Study participants were informed on their signed written consent form that their data would be used only for the study described on the consent form. FSL software packages from the FMRIB Software Library v6.0 were used in the analysis.

Acknowledgements

Funding for the work was provided by the REA of the European Commission through a Marie Curie Actions— International Incoming Fellowships (IIF) to Theodore Milner, project number 624431.

Appendix A. Supplementary data

Supplementary data to this article can be found online at https://doi.org/10.1016/j.ynirp.2022.100123.

References

Albert, N.B., Robertson, E.M., Miall, R.C., 2009. The resting human brain and motor learning. Curr. Biol. 19, 1023–1027.
Babadi, S., Vahdat, S., Milner, T.E., 2021. Neural substrates of muscle Co-contraction during dynamic motor adaptation. J. Neurosci. 41 (26), 5667–5676.

Binkofski, F.C., Klann, J., Caspers, S., 2016. On the neuroanatomy and functional role of the inferior parietal lobule and intraparietal sulcus. In: Neurobiology of Language. Academic Press, pp. 35–47.
Blakemore, S.-J., Wolpert, D.M., Frith, C.D., 1999. The cerebellum contributes to somatosensory cortical activity during self-produced tactile stimulation. Neuroimage 10, 448–459.
Bremmer, F., Schlack, A., Shah, N.J., Zafiris, O., Kubischik, M., Hoffmann, K.-P., Zilles, K., Fink, G.R., 2001. Polymodal motion processing in posterior parietal and premotor cortex: a human fMRI study strongly implies equivalencies between humans and monkeys. Neuron 29, 287–296.
Christensen, M.S., Lundbye-Jensen, J., Geertsen, S.S., Petersen, T.H., Paulson, O.B., Nielsen, J.B., 2007. Premotor cortex modulates somatosensory cortex during voluntary movements without proprioceptive feedback. Nat. Neurosci. 10, 417–419.
Cisek, P., Crammond, D.J., Kalaska, J.F., 2003. Neural activity in primary motor and dorsal premotor cortex in reaching tasks with the contralateral versus ipsilateral arm. J. Neurophysiol. 89, 922–942.
Desikan, R.S., Ségonne, F., Fischl, B., Quinn, B.T., Dickerson, B.C., Blacker, D., Buckner, R.L., Dale, A.M., Maguire, R.P., Hyman, B.T., 2006. An automated labeling system for subdividing the human cerebral cortex on MRI scans into gyral based regions of interest. Neuroimage 31, 968–980.
Diedrichsen, J., Balsters, J.H., Flavell, J., Cussans, E., Ramnani, N., 2009. A probabilistic MR atlas of the human cerebellum. Neuroimage 46, 39–46.
Ehrsson, H.H., Fagergren, A., Johansson, R.S., Forssberg, H., 2003. Evidence for the involvement of the posterior parietal cortex in coordination of fingertip forces for grasp stability in manipulation. J. Neurophysiol. 90, 2978–2986.
Eickhoff, S.B., Paus, T., Caspers, S., Grosbras, M.-H., Evans, A.C., Zilles, K., Amunts, K., 2007. Assignment of functional activations to probabilistic cytoarchitectonic areas revisited. Neuroimage 36, 511–521.
Farley, S.J., Radley, J.J., Freeman, J.H., 2016. Amygdala modulation of cerebellar learning. J. Neurosci. 36, 2190–2201.
Feinberg, D.A., Setsompop, K., 2013. Ultra-fast MRI of the human brain with simultaneous multi-slice imaging. J. Magn. Reson. 229, 90–100.
Fogassi, L., Luppino, G., 2005. Motor functions of the parietal lobe. Curr. Opin. Neurobiol. 15, 626–631.
Fox, M.D., Raichle, M.E., 2007. Spontaneous fluctuations in brain activity observed with functional magnetic resonance imaging. Nat. Rev. Neurosci. 8, 700–711.
Frey, S.H., Vinton, D., Norlund, R., Grafton, S.T., 2005. Cortical topography of human anterior intraparietal cortex active during visually guided grasping. Cognit. Brain Res. 23, 397–405.
Gallagher, M., Holland, P.C., 1994. The amygdala complex: multiple roles in associative learning and attention. Proc. Natl. Acad. Sci. USA 91, 11771–11776.
Greve, D.N., Fischl, B., 2009. Accurate and robust brain image alignment using boundary-based registration. Neuroimage 48, 63–72.
Harding, I.H., Yücel, M., Harrison, B.J., Pantelis, C., Breakspear, M., 2015. Effective connectivity within the frontoparietal control network differentiates cognitive control and working memory. Neuroimage 106, 144–153.
Hayward, V., Terekhov, A.V., Wong, S.-C., Geborek, P., Bengtsson, F., Jörntell, H., 2014. Spatio-temporal skin strain distributions evoke low variability spike responses in cuneate neurons. J. R. Soc. Interface 11, 20131015.
Herzfeld, D.J., Pastor, D., Haith, A.M., Rossetti, Y., Shadmehr, R., O'Shea, J., 2014. Contributions of the cerebellum and the motor cortex to acquisition and retention of motor memories. Neuroimage 98, 147–158.
Hsiao, S.S., O'shaughnessy, D., Johnson, K.O., 1993. Effects of selective attention on spatial form processing in monkey primary and secondary somatosensory cortex. J. Neurophysiol. 70, 444–447.
Imamizu, H., Miyauchi, S., Tamada, T., Sasaki, Y., Takino, R., PuÈtz, B., Yoshioka, T., Kawato, M., 2000. Human cerebellar activity reflecting an acquired internal model of a new tool. Nature 403, 192–195.
Imamizu, H., Kuroda, T., Miyauchi, S., Yoshioka, T., Kawato, M., 2003. Modular organization of internal models of tools in the human cerebellum. Proc. Natl. Acad. Sci. USA 100, 5461–5466.
Jäncke, L, Kleinschmidt, A, Mirzazade, S, Shah, N, Freund, H-J, 2001. The role of the inferior parietal cortex in linking the tactile perception and manual construction of object shapes. Cerebral Cortex 11, 114–121.
Jenkinson, M., Beckmann, C.F., Behrens, T.E., Woolrich, M.W., Smith, S.M., 2012. FSL. Neuroimage 62, 782–790.
Jiang, W., Tremblay, F., Chapman, C.E., 1997. Neuronal encoding of texture changes in the primary and the secondary somatosensory cortical areas of monkeys during passive texture discrimination. J. Neurophysiol. 77, 1656–1662.
Konkle, T., Wang, Q., Hayward, V., Moore, C.I., 2009. Motion aftereffects transfer between touch and vision. Curr. Biol. 19, 745–750.
Li, W., Qin, W., Liu, H., Fan, L., Wang, J., Jiang, T., Yu, C., 2013. Subregions of the human superior frontal gyrus and their connections. Neuroimage 78, 46–58.
Lutkenhoff, E.S., Rosenberg, M., Chiang, J., Zhang, K., Pickard, J.D., Owen, A.M., Monti, M.M., 2014. Optimized brain extraction for pathological brains (optiBET). PLoS One 9, e115551.
Manzoni, T., Conti, F., Fabri, M., 1986. Callosal projections from area SII to SI in monkeys: anatomical organization and comparison with association projections. J. Comp. Neurol. 252, 245–263.
Nezafat, R., Shadmehr, R., Holcomb, H.H., 2001. Long-term adaptation to dynamics of reaching movements: a PET study. Exp. Brain Res. 140, 66–76.
Petit, G., Dufresne, A., Levesque, V., Hayward, V., Trudeau, N., 2008. Refreshable tactile graphics applied to schoolbook illustrations for students with visual impairment. In: Proceedings of the 10th International ACM SIGACCESS Conference on Computers and Accessibility, pp. 89–96.
Pleger, B., Foerster, A.-F., Ragert, P., Dinse, H.R., Schwenkreis, P., Malin, J.-P., Nicolas, V., Tegenthoff, M., 2003. Functional imaging of perceptual learning in human primary and secondary somatosensory cortex. Neuron 40, 643–653.
Pleger, B., Ruff, C.C., Blankenburg, F., Bestmann, S., Wiech, K., Stephan, K.E., Capilla, A., Friston, K.J., Dolan, R.J., 2006. Neural coding of tactile decisions in the human prefrontal cortex. J. Neurosci. 26, 12596–12601.
Rao, S.M., Binder, J., Bandettini, P., Hammeke, T., Yetkin, F., Jesmanowicz, A., Lisk, L., Morris, G., Mueller, W., Estkowski, L., 1993. Functional magnetic resonance imaging of complex human movements. Neurology 43, 2311-2311.
Reed, C.L., Klatzky, R.L., Halgren, E., 2005. What vs. where in touch: an fMRI study. Neuroimage 25, 718–726.
Ricciardi, E., Vanello, N., Sani, L., Gentili, C., Scilingo, E.P., Landini, L., Guazzelli, M., Bicchi, A., Haxby, J.V., Pietrini, P., 2007. The effect of visual experience on the development of functional architecture in hMT+. Cerebr. Cortex 17, 2933–2939.
Romo, R., Hernández, A., Zainos, A., Lemus, L., Brody, C.D., 2002. Neuronal correlates of decision-making in secondary somatosensory cortex. Nat. Neurosci. 5, 1217–1225.
Rossi-Pool, R., Zainos, A., Alvarez, M., Zizumbo, J., Vergara, J., Romo, R., 2017. Decoding a decision process in the neuronal population of dorsal premotor cortex. Neuron 96, 1432–1446.
Sakata, H., Taira, M., Murata, A., Mine, S., 1995. Neural mechanisms of visual guidance of hand action in the parietal cortex of the monkey. Cerebr. Cortex 5, 429–438.
Sani, L., Ricciardi, E., Gentili, C., Vanello, N., Haxby, J.V., Pietrini, P., 2010. Effects of visual experience on the human MT+ functional connectivity networks: an fMRI study of motion perception in sighted and congenitally blind individuals. Front. Syst. Neurosci. 4, 159.
Sathian, K., Deshpande, G., Stilla, R., 2013. Neural changes with tactile learning reflect decision-level reweighting of perceptual readout. J. Neurosci. 33, 5387–5398.
Schmitz, C., Jenmalm, P., Ehrsson, H.H., Forssberg, H., 2005. Brain activity during predictable and unpredictable weight changes when lifting objects. J. Neurophysiol. 93, 1498–1509.
Setsompop, K., Gagoski, B.A., Polimeni, J.R., Witzel, T., Wedeen, V.J., Wald, L.L., 2012. Blipped-controlled aliasing in parallel imaging for simultaneous multislice echo planar imaging with reduced g-factor penalty. Magn. Reson. Med. 67, 1210–1224.
Shadmehr, R., Holcomb, H.H., 1997. Neural correlates of motor memory consolidation. Science 277, 821–825.
Shehzad, Z., Kelly, A.C., Reiss, P.T., Gee, D.G., Gotimer, K., Uddin, L.Q., Lee, S.H., Margulies, D.S., Roy, A.K., Biswal, B.B., 2009. The resting brain: unconstrained yet reliable. Cerebr. Cortex 19, 2209–2229.
Smith, S.M., Jenkinson, M., Woolrich, M.W., Beckmann, C.F., Behrens, T.E., Johansen-Berg, H., Bannister, P.R., De Luca, M., Drobnjak, I., Flitney, D.E., 2004. Advances in functional and structural MR image analysis and implementation as FSL. Neuroimage 23, S208–S219.
Stoesz, M.R., Zhang, M., Weisser, V.D., Prather, S., Mao, H., Sathian, K., 2003. Neural networks active during tactile form perception: common and differential activity during macrospatial and microspatial tasks. Int. J. Psychophysiol. 50, 41–49.
Strick, P.L., Dum, R.P., Fiez, J.A., 2009. Cerebellum and nonmotor function. Annu. Rev. Neurosci. 32, 413–434.
Sutherland, M.T., Tang, A.C., 2006. Reliable detection of bilateral activation in human primary somatosensory cortex by unilateral median nerve stimulation. Neuroimage 33, 1042–1054.
Thura, D., Cisek, P., 2014. Deliberation and commitment in the premotor and primary motor cortex during dynamic decision making. Neuron 81, 1401–1416.
Tunik, E., Frey, S.H., Grafton, S.T., 2005. Virtual lesions of the anterior intraparietal area disrupt goal-dependent on-line adjustments of grasp. Nat. Neurosci. 8, 505–511.
Tziortzi, A.C., Searle, G.E., Tzimopoulou, S., Salinas, C., Beaver, J.D., Jenkinson, M., Laruelle, M., Rabiner, E.A., Gunn, R.N., 2011. Imaging dopamine receptors in humans with [11C]-(+)-PHNO: dissection of D3 signal and anatomy. Neuroimage 54, 264–277.
Vahdat, S., Darainy, M., Ostry, D.J., 2014. Structure of plasticity in human sensory and motor networks due to perceptual learning. J. Neurosci. 34, 2451–2463.
Vahdat, S., Darainy, M., Milner, T.E., Ostry, D.J., 2011. Functionally specific changes in resting-state sensorimotor networks after motor learning. J. Neurosci. 31, 16907–16915.
van Boven, R.W., Ingeholm, J.E., Beauchamp, M.S., Bikle, P.C., Ungerleider, L.G., 2005. Tactile form and location processing in the human brain. Proc. Natl. Acad. Sci. USA 102, 12601–12605.
van Vugt, F.T., Near, j, Hennesey, T., Doyon, J., Ostry, D.J., 2020. Early stages of sensorimotor map acquisition: neurochemical signature in primary motor cortex and its relation to functional connectivity. J. Neurophysiol. 124, 1615–1624.
Wacker, E., Spitzer, B., Lützkendorf, R., Bernarding, J., Blankenburg, F., 2011. Tactile motion and pattern processing assessed with high-field FMRI. PLoS One 6, e24860.
Wang, Q., Hayward, V., 2010. Biomechanically optimized distributed tactile transducer based on lateral skin deformation. Int. J. Robot Res. 29, 323–335.
Woolrich, M.W., Ripley, B.D., Brady, M., Smith, S.M., 2001. Temporal autocorrelation in univariate linear modeling of FMRI data. Neuroimage 14, 1370–1386.
Woolrich, M.W., Behrens, T.E., Beckmann, C.F., Jenkinson, M., Smith, S.M., 2004. Multilevel linear modelling for FMRI group analysis using Bayesian inference. Neuroimage 21, 1732–1747.
Zhang, Y., Brady, M., Smith, S., 2001. Segmentation of brain MR images through a hidden Markov random field model and the expectation-maximization algorithm. IEEE Trans. Med. Imag. 20, 45–57.